ACS OMEGA

Open Access

http://pubs.acs.org/journal/acsodf

Article

Simulation and Analysis of a Novel Hydrogen Liquefaction Process Based on the Liquid Nitrogen and Helium Joule−Brayton Cycle

Wenhao Song,* Ke Liu, Zhonghua Zhao, Limeng Zhang, Xinguang Dong, Xingsen Yang, Chunxiao Tian, Shuai Liu, and Shuo Cao

Cite This: *ACS Omega* 2025, 10, 8089−8102

Read Online

ACCESS | Metrics & More | Article Recommendations

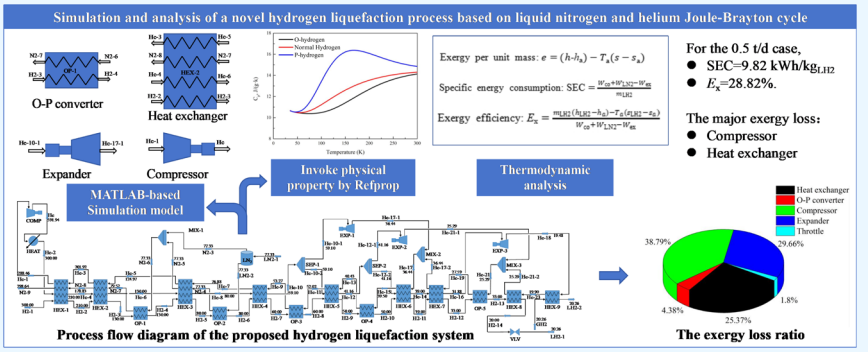

ABSTRACT: To facilitate the design, analysis, and optimization of the hydrogen liquefaction system, this study developed a MATLAB-based independent simulation program encompassing unit equipment models and exergy analysis models. The program incorporated REFPROP software to accurately calculate fluid physical properties and the heat of conversion between ortho- and parahydrogen. The proposed hydrogen liquefaction process utilized LN_2 precooling, the helium Joule−Brayton cryogenic cycle, and a throttle valve to efficiently produce liquid hydrogen. The simulation results were rigorously validated using the industry standard Unisim Design software. For the 0.5 t/d hydrogen liquefaction system, the exergy efficiency stood at 28.82%, accompanied by a specific energy consumption of 9.82 kW h/kg$_{LH2}$. Notably, the compressor contributed the highest exergy loss ratio, accounting for 38.79% of the total. Increasing the compressor efficiency could significantly improve the exergy efficiency and reduce energy consumption. A comparative analysis revealed that at a larger scale of 50 t/d, the exergy losses of both the compressor and expander decreased, whereas the heat exchanger accounted for 36.29% of the total. In conclusion, the independent simulation program established in this study served as a valuable tool for simulating and analyzing the hydrogen liquefaction system, providing a crucial reference for design improvements and optimization efforts.

1. INTRODUCTION

As a versatile energy carrier that can be derived from diverse sources, hydrogen stands as a crucial bridge in the transition from fossil fuels to renewable energy, heralding novel transformations in the realm of clean energy utilization.[1] Amidst the introduction and implementation of the ambitious goals of "carbon peaking" and "carbon neutrality", over 20 nations and economic systems, including the United States,[2] China,[3] Germany,[4] Japan,[5] etc., have unveiled national strategies for hydrogen energy. Within the application of hydrogen energy, addressing challenges spanning production, storage, transportation, and utilization is paramount, with storage and transportation being pivotal components for its widespread adoption. At present, compared with immature chemical hydrogen storage, mature hydrogen storage and transportation methods mainly include high-pressure gas hydrogen and liquid hydrogen. Gas hydrogen needs to be pressurized to 35−70 MPa, but the increase of energy density is still limited (density 39.05 kg/m^3, 70 MPa at 300 K). Liquid hydrogen has high energy density (density 70.85 kg/m^3, 0.1 MPa @ 20 K), low storage pressure, and high purity.[6] However, the cost of hydrogen liquefaction restricts further application of liquid hydrogen. Given considerations such as hydrogen storage density, economy, and safety, it is anticipated that liquid hydrogen could emerge as a primary means for large-scale storage and transportation, provided that the

Received: October 11, 2024
Revised: January 23, 2025
Accepted: February 12, 2025
Published: February 22, 2025

efficiency of hydrogen liquefaction undergoes further enhancement.

The principle of large-scale hydrogen liquefaction plants[7] commonly is based on the Linde−Hampson liquefaction cycle,[8,9] helium Joule−Brayton liquefaction cycle,[10] and Claude liquefaction cycle,[11] including the ortho−parahydrogen conversion to meet the long-term storage requirements of liquid hydrogen.[12,13] The Linde−Hampson cycle has the characteristics of a simple process, low efficiency, and high energy consumption, suitable for small hydrogen liquefaction units at the laboratory level. The Joule−Brayton helium cycle uses a helium turbine expander. Compared with the hydrogen expander used in the Claude cycle, helium is an inert gas, which avoids safety risks such as hydrogen embrittlements, hydrogen leakage, and polyphase expansion. In addition, liquid nitrogen (LN2) is easy to obtain, and the throttle valve is simple and stable. The remarkable feature of the proposed process is that it is expected to be applied in large-scale engineering under the conditions of existing technology and equipment. At present, the specific energy consumption (SEC) of large-scale hydrogen liquefaction plants in operation is 10−15 kW h/kg_{LH2}, and the exergy efficiency is only 20−30%. The actual representative plants are Linde's large-scale hydrogen liquefaction plants in Ingolstadt and Leuna, Germany, with a capacity of 5 t/d and an SEC of 13.6 and 11.9 kW h/kg_{LH2}, respectively.[14,15] The plants operated by Praxair have a production capacity of 18−30 t/d, with an SEC ranging from approximately 12.5−15 kW h/kg_{LH2}.[10,16]

There are a series of challenges in the hydrogen liquefaction system, including wide temperature range, complex process, high energy consumption, and low efficiency.[17,18] With the escalating demand for hydrogen energy, the research focus in recent years has shifted toward optimizing the overall performance of the hydrogen liquefaction system. In the exploration of large-scale conceptual devices, initial efforts were directed toward enhancing the thermodynamic cycle, subsequently shifting to improvements in the composition and performance of refrigerant, and the current trend is heavily focused on the integration and optimization of both aspects. Kuz'Menko[19] refined the hydrogen liquefaction system designed by Belyakov,[20] introducing an enhanced LN2 precooling device and a helium Joule−Brayton cycle. This modified system boasted a production capacity of 54 t/day, elevating the exergy efficiency by 6% and achieving an SEC of 12.7 kW h/kg_{LH2}. Valenti designed a four-stage helium Joule−Brayton cycle. The helium refrigeration cycle was applied in both the precooling stage and cryogenic stage, and the SEC of the system was 5.8 kW h/kg_{LH2}.[21] The refrigeration of a mixed refrigerant with low energy consumption has become a hot research spot of hydrogen liquefaction recently.[22] Since the boiling points of the mixed refrigerant components are different, the endothermic boiling process is a variable temperature process, so the temperature difference between heat flow and cold flow in the heat exchanger is relatively low, which reduces the cooling loss and improves the exergy efficiency. Sadaghiani[23] opted for the ideal mixed refrigerant in the precooling stage and cryogenic stage. Moreover, the integration of the heat exchanger and expander suitable for a wide temperature range contributed to an SEC of 4.4 kW h/kg_{LH2} and an energy efficiency of 55.5%. Zhang and Liu[24] implemented a mixed refrigerant Claude liquefaction cycle for the precooling stage, along with a nitrogen and two other mixed refrigerants Joule−Brayton cycle for the cryogenic stage, creating a four-stage independent cycle. This plant boasted a production capacity of 288.9 t/day with an SEC of 5.9 kW h/kg_{LH2} and an exergy efficiency of 55.3%. Bi[25] optimized the components of the mixed refrigerant in the precooling cycle through genetic algorithm. The study results showed that the SEC at 5 t/day could be reduced to 9.7 kW h/kg_{LH2}, with an exergy efficiency of 39.1%. Faramarzi[26] proposed a hydrogen liquefaction process with LNG precooling and a mixed refrigerant cryogenic cycle. The feedstock hydrogen was cooled to 131 K by the cold energy of LNG vaporization, then cooled to 20 K, and converted into liquid hydrogen through the cryogenic cycle with a mixture of helium, hydrogen, and neon, where the SEC was reduced by 34% compared to Ansarinasab.[27] Naquash[28] added hydrofluoroolefin into the mixed refrigerant to improve the exergy efficiency, reducing the SEC of the precooling cycle by 41.8%, but the equipment investment cost also increased significantly.

At present, the SEC of a large-scale commercial hydrogen liquefaction plant is generally high (12.5−15 kW h/kg_{LH2}). In the above literature studies, most of these efficient solutions are based on the premise of improving equipment efficiency and production capacity and have not been applied in practice. In addition, some of the simulations lack accurate physical property data of O-hydrogen and P-hydrogen and ignore the ortho−parahydrogen conversion reaction or adopt approximate means to simulate the conversion process.[21,23] In this study, REFPROP V10.0 is invoked to obtain accurate physical properties of the O-hydrogen and P-hydrogen and realize equilibrium hydrogen physical property calculation and simulation of ortho−parahydrogen conversion. By integrating the unit equipment models, the independent and flexible simulation program based on Matlab is developed. A simple and efficient hydrogen liquefaction process incorporating LN_2 precooling, helium Joule−Brayton cycle, and final-stage throttling was proposed. The results of this simulation were further corroborated through commercial software validation, and a comprehensive analysis of energy consumption and exergy loss was presented. This study is expected to realize large-scale engineering application under the condition of existing technology and equipment, providing reference for the design, simulation, and optimization of hydrogen liquefaction system.

2. THEORETICAL BASIS

2.1. Process Description. According to the fundamental design principles of industrial production, encompassing adaptability, cost-efficiency, reliability, technological advancement, flexibility, and simplicity, the precooling, cryogenic cycle, and liquefaction stage of the hydrogen liquefaction system were designed successively. Specifically, for a capacity below 5 t/d, the design principle of a simple refrigeration process and stable operation should be followed, while also taking into account energy consumption.

In this liquefaction system, the precooling process used LN_2, while the cryogenic process utilized the helium Joule−Brayton cycle. The choice of helium as a refrigerant could avoid numerous technical challenges associated with the Claude liquefaction cycle. First, helium, as an inert gas, poses minimal environmental risk in the event of a leak and does not corrode equipment. Second, helium remains in its gaseous state throughout the temperature range of the liquefaction system, thus eliminating issues related to polyphase expansion. Moreover, the helium expander, which is commonly employed

https://doi.org/10.1021/acsomega.4c09299
ACS Omega 2025, 10, 8089−8102

in helium liquefaction systems, exhibits greater efficiency than the hydrogen expander.

The liquefaction system exhibits a direct correlation between the number of expansion stages and its SEC, with an increasing number of stages resulting in lower SEC and higher thermodynamic efficiency. However, an excessive number of expansion stages can introduce complexities to the process, thereby diminishing the stability and reliability of the liquefaction system. Additionally, it can lead to an increase in the equipment cost and maintenance requirement. Consequently, the helium Joule−Brayton cycle in this liquefaction system has been designed to employ a three-stage expansion. The feed hydrogen, undergoing the precooling and cryogenic process, was typically converted into liquid hydrogen through throttle expansion and then directly routed into the liquid hydrogen storage tank, such as Linde's hydrogen liquefaction plants in Ingelstadt and Leuna.[14] In this study, a straightforward and reliable throttle valve was also employed to achieve hydrogen liquefaction.

During the cooling process, the constant-pressure specific heat of hydrogen undergoes substantial variations, especially below 2 MPa. To minimize heat-transfer losses resulting from this dramatic change, the pressure of the feed hydrogen should also be increased as much as possible. In addition, Quack[29] has emphasized that increasing the pressure of feed hydrogen was beneficial in terms of SEC. However, this higher pressure posed significant challenges in the design and development of hydrogen compressors, while also posing potential safety risks to the liquefaction system. Considering the influence of pressure on the plate-fin heat exchanger and expander, the pressure of feed hydrogen in this study was selected as the conventional operating parameter, 2.1 MPa. For the hydrogen liquefaction system with the helium Joule−Brayton cycle, it was not sensitive to variations in helium pressure when the pressure was maintained at approximately 1 MPa.[30] Consequently, the helium pressure was selected as 1.2 MPa in this study. Based on pertinent research studies,[31,32] the helium compressor's efficiency ranged from 0.65 to 0.8, while the turbine expander's isentropic efficiency ranged from 0.75 to 0.85. Notably, both compressor and expander efficiencies increased with an increasing system scale. In this study, for a liquefaction system of 0.5 t/d, the helium compressor and expander efficiencies were selected as 70% and 75%, respectively.

There exist two distinct spin isomers of hydrogen:[33] orthohydrogen (O-hydrogen) and parahydrogen (P-hydrogen), as shown in Figure 1. At a standard temperature, the O-hydrogen constitutes approximately 75% of the total hydrogen content, while the P-hydrogen accounts for the remaining 25%. As the temperature decreases, a spontaneous conversion of O-hydrogen to the oxygen occurs in hydrogen, aiming to establish a new equilibrium state. This ortho−parahydrogen conversion is characterized as a slow exothermic reaction. However, if this reaction takes place within a liquid hydrogen storage tank, approximately 50% of liquid hydrogen evaporates within 10 days due to the fact that the heat released by the reaction (527 kJ/kg)[34] surpasses the latent heat of vaporization of liquid hydrogen (443 kJ/kg).[35] The heat of conversion of the O-hydrogen to the P-hydrogen is as shown in Figure 2. To avoid this issue, it is necessary to add a reaction catalyst to the liquefaction system to speed up the conversion.

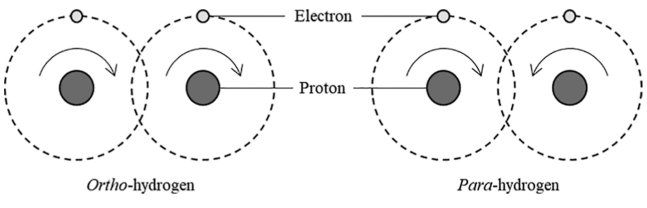

Figure 1. Configuration of O-hydrogen and P-hydrogen.

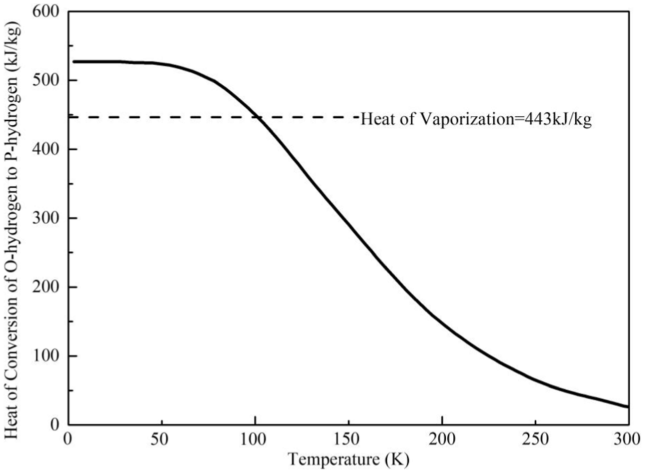

Figure 2. Heat of conversion of O-hydrogen to P-hydrogen.

Integrating the heat exchanger with the catalyst actually brings the conversion process closer to the ideal of a continuous, minimal energy consumption process. Nevertheless, this approach faces challenges such as complex structural design, requirement of a large amount of catalyst, and high airflow resistance. Given the costs associated with processing and manufacturing, most hydrogen liquefaction systems opt for a multistage ortho−parahydrogen conversion approach as a means to approximate the ideal continuous conversion. This liquefaction system incorporated a five-stage ortho−parahydrogen conversion to emulate the conversion reaction. The reaction in the reactor is as follows

$$\text{O-hydrogen} \rightarrow \text{P-hydrogen} + \text{heat}$$

In summary, the process flow diagram of the proposed hydrogen liquefaction system is shown in Figure 3, and the selection of hydrogen liquefaction process parameters is shown in Table 1. The liquefaction system incorporated three distinct fluids: circulating helium, feed hydrogen, and LN_2. Recycled helium and LN_2 served as refrigerants, effectively cooling feed hydrogen. Within the helium Joule−Brayton cycle, low-pressure helium was pressurized by a compressor (COMP) and cooled to room temperature via a heat exchanger (HEX). This helium then traversed heat exchangers HEX1, HEX2, and HEX3, reaching a temperature of approximately 77 K through the combined cooling of low-temperature helium and LN_2. Further cooling occurred in heat exchangers HEX4, HEX5, HEX6, and HEX7, where the helium was divided into three streams and expanded to 0.2 MPa through expanders EXP-1, EXP-2, and EXP-3. The resulting low-pressure, low-temperature helium then provided cooling for heat exchangers HEX8 to HEX1 in sequence. LN_2 provided the cooling through the ortho−parahydrogen conversion reactor (O−P converter) OP-2, heat exchanger HEX3, O−P converter OP-1, heat exchanger HEX2, and heat exchanger HEX1 in turn. After passing

https://doi.org/10.1021/acsomega.4c09299
ACS Omega 2025, 10, 8089−8102

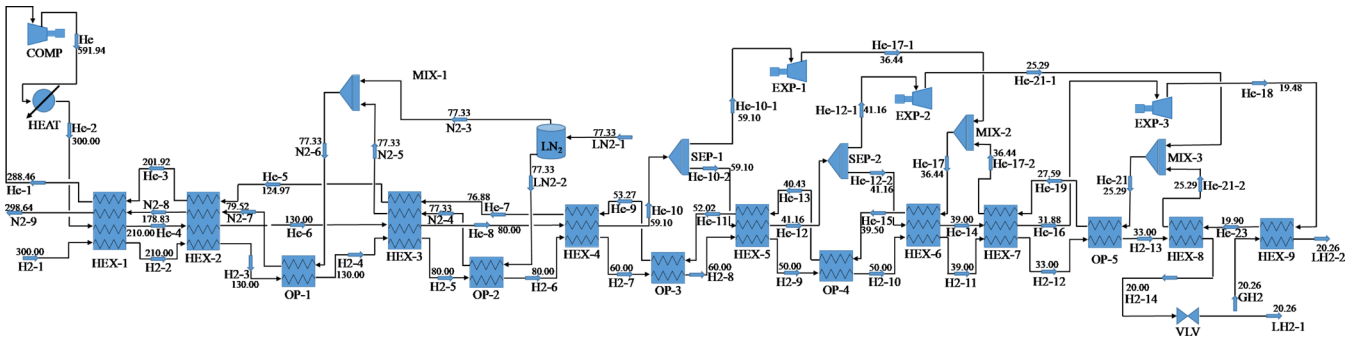

Figure 3. Process flow diagram of the proposed hydrogen liquefaction system.

Table 1. Selection of Process Parameters for the Hydrogen Liquefaction System

item	numerical value
capacity (t/d)	0.5
H2 feed pressure (MPa)	2.1
H2 feed temperature (K)	300
LH_2 product pressure (MPa)	0.1
LH_2 product temperature (K)	20.2
LH_2 product P-hydrogen fraction (%)	>95
efficiency of compressors (%)	70
efficiency of expander (%)	75
ortho−parahydrogen conversion	5 stages

through heat exchangers HEX1 ∼ HEX8 and O−P converters OP-1 ∼ OP-4 in turn, the feed hydrogen was cooled down to about 20 K by LN2 and low-pressure helium. Subsequently, it was throttled to 0.1 MPa through a throttle valve (VLV), forming a gas−liquid two-phase. This generated flash hydrogen was further liquefied in HEX9 and entered the liquid hydrogen storage tank. In this liquefaction system, it was considered to reduce the feed hydrogen temperature before throttling as much as possible, so as to reduce throttling loss and simplify the process.

2.2. Methodology and Building. The thermodynamic submodel for unit equipment was crafted utilizing MATLAB software, and the overall liquefaction system model was further integrated. Furthermore, REFPROP was utilized to obtain and invoke crucial physical property data. Next, the thermodynamic submodel of the system was elaborated in detail. For the convenience of analysis, the hydrogen liquefaction system was simplified based on the following assumptions:

(1) The pipeline and heat exchanger's flow pressure drop and heat leakage were disregarded;
(2) The power of the expansion machine could be recovered, and the mechanical power-transfer efficiency was assumed to be 100%;
(3) The ortho−parahydrogen conversion occurred exclusively within the reactors and could eventually reach the equilibrium at the corresponding temperature;
(4) The system was assumed to be in a steady state, ignoring the influence of kinetic energy and potential energy;
(5) The minimum logarithmic mean temperature difference (LMTD) in the multistream heat exchanger was ≥0.5 K.

$$\text{LMTD: } \Delta t_m = \frac{\Delta t_{max} - \Delta t_{min}}{\ln \frac{\Delta t_{max}}{\Delta t_{min}}} \quad (1)$$

For a detailed analysis of the liquefaction system, an exergy assessment of all components has been conducted, encompassing both the quantity and the quality of energy. Exergy, a state parameter that is comprehensively addressed by the first and second laws of thermodynamics, offers an objective and unified evaluation of the overall performance of a hydrogen liquefaction system.[36] It further pinpoints the location and magnitude of the energy losses. These exergy losses encompass external losses flowing directly to the environment, as well as internal losses arising from the irreversibility in the actual process.[37] The exergy loss of each component could be precisely determined by solving the exergy balance equation. The detailed formulas are as follows

$$\text{Exergy per unit mass: } e = (h - h_a) - T_a(s - s_a) \quad (2)$$

$$\text{Exergy loss: } \Delta E = \sum E_{in} - \sum E_{out} \quad (3)$$

$$\text{Exergy loss ratio: } r_i = \frac{\Delta E_i}{\sum \Delta E_i} \quad (4)$$

In the formula, h (kJ/kg) and s (kJ/(kg·K)) are the enthalpy and entropy of the fluid in a specific state, respectively; h_a and s_a are the enthalpy and entropy of the fluid in an environmental state, respectively. T_a is the environmental temperature, K. E_{in} is for the inlet exergy of the fluid, and E_{out} is for the outlet exergy of the fluid, kW. ΔE_i is the exergy loss of unit equipment i, and r_i is the exergy loss ratio of unit equipment i.

The liquefaction system is typically evaluated by using two key systematic indices: SEC and exergy efficiency. SEC is the ratio of total system energy consumption to liquid hydrogen capacity. Exergy efficiency is the ratio of theoretical minimum energy consumption to actual energy consumption. This efficiency measure reflects the irreversibility of the liquefaction system, where higher exergy efficiency indicates the lower energy loss and more economy. The detailed formulas are as follows

$$\text{Specific energy consumption: } SEC = \frac{W_{co} + W_{LN2} - W_{ex}}{m_{LH2}} \quad (5)$$

$$\text{Exergy efficiency: } E_x = \frac{m_{LH2}(h_{LH2} - h_a) - T_a(s_{LH2} - s_a)}{W_{co} + W_{LN2} - W_{ex}} \quad (6)$$

In the formula, W_{LN2} is the energy consumption of LN_2, kW; W_{co} is the energy consumption of the compressor, kW; W_{ex} is the output power of the expander, kW; m_{LH2} is the hydrogen

https://doi.org/10.1021/acsomega.4c09299
ACS Omega 2025, 10, 8089−8102

liquefaction flow rate, kg/s; h_{LH2} and s_{LH2} are the enthalpy and entropy of liquid hydrogen, kJ/kg and kJ/(kg·K), respectively.

The following is an analysis of the energy and exergy losses of key equipment in the hydrogen liquefaction system. The compressor, as a critical moving component in the liquefaction system, significantly affects the overall energy consumption. Helium is initially compressed by a compressor to achieve high pressure and then cooled to room temperature within a heat exchanger. The detailed formulas are as follows

Isentropic efficiency of the compressor i: η_{coi}

$$= \frac{h_{outs,coi} - h_{in,coi}}{h_{out,coi}\text{-}h_{in,coi}} \tag{7}$$

Power consumption of the compressor i: W_{coi}

$$= \frac{m_{coi}((h_{out,coi}\text{-}h_{in,coi}) - T_a(s_{out,coi}\text{-}s_{in,coi}))}{\eta_{coi}} \tag{8}$$

Exergy loss of compress i: ΔE_{coi}

$$= E_{in} - E_{out}$$
$$= m_{coi}(e_{in,coi} - e_{out,coi}) + W_{coi} \tag{9}$$

In the formula, n_{coi} is the compressor efficiency i; $h_{in,coi}$ and $h_{out,coi}$ are the specific enthalpies of the inlet and outlet fluid, kJ/kg, respectively; $h_{outs,\ coi}$ is the specific enthalpy of the outlet fluid under the ideal condition; W_{coi} is the energy consumption of compressor i; m_{coi} is the compressor flow rate, kg/s; $s_{in,coi}$ and $s_{out,coi}$ are the specific enthalpies of the inlet and outlet fluid, kJ/(kg·K), respectively; and $e_{in,coi}$ and $e_{out,coi}$ are the specific exergies of the inlet and outlet fluid, kJ/(kg·K), respectively.

Helium expansion refrigeration is a key source of hydrogen cooling energy below 80 K. The helium expansion process is approximated as an isentropic expansion. The detailed formulas are as follows

Isentropic efficiency of the expander i: η_{exi}

$$= \frac{h_{in,exi} - h_{out,exi}}{h_{in,exi} - h_{outs,exi}} \tag{10}$$

Output power of the expander i: W_{exi}

$$= m_{exi}(h_{in,exi} - h_{out,exi}) \tag{11}$$

Output power of the expanders: $W_{ex} = \sum W_{exi}$ (12)

Exergy loss of the expander i: ΔE_{exi}

$$= E_{in} - E_{out}$$
$$= m_{exi}(e_{in,exi} - e_{out,exi}) - W_{exi} \tag{13}$$

Exergy loss of the expanders: $\Delta E_{ex} = \sum E_{exi}$ (14)

In the formula, $h_{in,exi}$ and $h_{out,exi}$ are the specific enthalpies of the inlet and outlet fluid, kJ/kg, respectively; $h_{outs,\ exi}$ is the specific enthalpy of the outlet fluid under the ideal isentropic condition; W_{exi} is the power consumption of expander i; m_{exi} is the expander flow rate, kg/s; and $e_{in,exi}$ and $e_{out,exi}$ are the specific exergies of the inlet and outlet fluid, kJ/(kg·K), respectively.

Throttling is the last stage of hydrogen liquefaction, which is an isoenthalpy process. Low-temperature hydrogen is converted to liquid hydrogen in the throttle valve. The detailed formulas are as follows

Valve: $m_{in}h_{in,vlv} = m_{GH2}h_{GH2,vlv} + m_{LH2}h_{LH2,vlv}$ (15)

Exergy loss of valve: ΔE_{vlv}

$$= E_{in} - E_{out}$$
$$= m_{in}e_{in,vlv} - m_{GH2}e_{GH2,vlv} - m_{LH2}e_{LH2,vlv} \tag{16}$$

In the formula, $h_{in,vlv}$ $e_{in,vlv}$ is the specific enthalpy and exergy of the inlet hydrogen, kJ/kg, respectively; $h_{GH2,vlv}$ and $h_{LH2,vlv}$ are the specific enthalpies of the outlet fluid, GH2 and LH2, kJ/kg, respectively; and $e_{GH2,vlv}$ and $e_{LH2,vlv}$ are the specific exergies of the outlet fluid, GH2 and LH2, kJ/kg, respectively.

The multistream heat exchanger is the most common unit equipment in the hydrogen liquefaction system, following the energy conservation principle during the heat-exchange process. In existing studies on hydrogen liquefaction,[38,39] the commonly used formula is as follows

Heat exchangers: $\sum m_{hi}c_{p,hi}(T_{in,hi} - T_{out,hi})$
$$= \sum m_{cj}c_{p,cj}(T_{out,cj} - T_{in,cj}) \tag{17}$$

In the formula, m_{cj} and m_{hi} are the flow rates of cold fluid j and hot fluid i, kg/s, respectively; $c_{p,c}$ and $c_{p,hi}$ are the specific heat of cold fluid j and hot fluid i, kJ/(kg·K), respectively; $T_{in,hi}$ and $T_{out,hi}$ are the inlet and outlet temperatures of hot fluid i, K; and $T_{out,ci}$ and $T_{in,ci}$ are the inlet and outlet temperatures of cold fluid j, K.

The profiles of heat capacities of hydrogen as a function of temperature are as shown in Figure 4.[33] Due to the

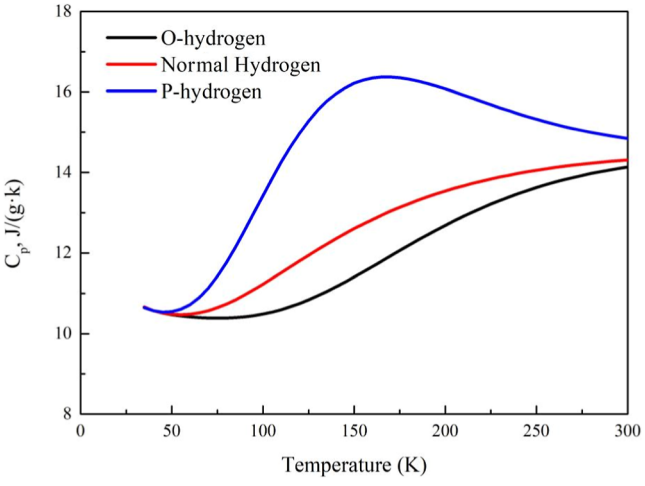

Figure 4. Profiles of heat capacities of hydrogen as a function of temperature.

temperature-dependent variation in the specific heat of fluids, and the deviation of hydrogen's physical properties from the ideal gas at low temperature, heat-transfer calculation using the specific heat often resulted in significant deviations. To address this issue, this study adopted the enthalpy difference as the fundamental basis for heat-transfer calculation, thereby ensuring greater accuracy in the computations. The detailed formulas are as follows

https://doi.org/10.1021/acsomega.4c09299
ACS Omega 2025, 10, 8089−8102

$$\text{Heat exchangers: } \sum m_{h,i}(h_{in,hi} - h_{out,hi}) = \sum m_{c,j}(h_{out,cj} - h_{in,cj}) \quad (18)$$

$$\text{Exergy loss of heat exchanger: } \Delta E_{HX} = E_{in} - E_{out} = \sum_{i=1}^{n} m_i(e_{in,i} - e_{out,i}) \quad (19)$$

In the formula, $h_{in,hi}$ and $h_{out,hi}$ are the specific enthalpies of the inlet and outlet hot fluid i, kJ/(kg·K), respectively; $h_{in,cj}$ and $h_{out,cj}$ are the specific enthalpies of the inlet and outlet cold fluid j, kJ/(kg·K), respectively; m_i is the fluid i flow rate, kg/s; and $e_{in,i}$ and $e_{out,i}$ are the specific exergy of the inlet and outlet fluid i, kJ/(kg·K), respectively.

Give an example, for the heat exchanger HEX-2, as shown in Figure 5, He-4 and He-6 represent the inlet and outlet high-temperature helium, He-5 and He-3 represent the inlet and outlet low-temperature reflux helium, H2−2 and H2−3 represent the inlet and outlet hydrogen, and N2−7 and N2−8, respectively, represent the inlet and outlet low-temperature nitrogen, respectively. Energy conservation equation and exergy loss calculation formula are as follows

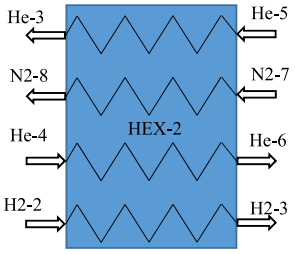

Figure 5. Schematic diagram of the inlet and outlet fluids in heat exchanger HEX-2.

$$m_{H2}(h_{H2-2} - h_{H2-3}) + m_{He}(h_{He-4} - h_{He-6}) = m_{N2}(h_{N2-8} - h_{N2-7}) + m_{He}(h_{He-3} - h_{He-5}) \quad (20)$$

$$\Delta E_{HEX-2} = E_{in} - E_{out} = m_{H2}(e_{H2-2} - e_{H2-3}) + m_{N2}(e_{N2-7} - e_{N2-8}) + m_{He}(e_{He-4} + e_{He-5} - e_{H2-6} - e_{H2-3}) \quad (21)$$

For the O−P converter OP-1, as shown in Figure 6, H2−3 and H2−4 represent the inlet and outlet hydrogen, and N2−6 and N2−7 represent the inlet and outlet low-temperature nitrogen, respectively. Energy conservation equation and exergy loss calculation formula are as follows

$$m_{H2}(h_{H2-3} - h_{H2-4}) = m_{N2}(h_{N2-7} - h_{N2-6}) \quad (22)$$

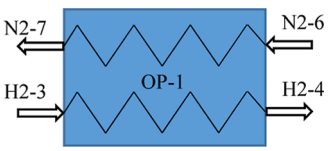

Figure 6. Schematic diagram of the inlet and outlet fluids in O−P converter OP-1.

$$\Delta E_{OP-1} = E_{in} - E_{out} = m_{H2}(e_{H2-3} - e_{H2-4}) + m_{N2}(e_{N2-6} - e_{N2-7}) \quad (23)$$

Due to the wide temperature range in the hydrogen liquefaction system, the working fluids include gas phase, liquid phase, and two phases. Therefore, reliable physical property data are essential to ensure the accuracy of simulation. The physical property databases used in this project include helium (He), nitrogen (N2), normal hydrogen (H2), orthohydrogen (O−H2), and Parahydrogen (P−H2), which are obtained by calling REFPROP V10.0. During the cooling process, the P-hydrogen fraction of feed hydrogen changes continuously, and its physical properties are close to those of equilibrium hydrogen at the corresponding temperature. REFPROP 10.0 offers comprehensive physical property data for both O-hydrogen and P-hydrogen. Through invoking the REFPROP physical property database, the entropy and enthalpy of equilibrium hydrogen at a given temperature, pressure, and P-hydrogen fraction could be calculated. The calculation formulas are as follows[40]

$$h_{mix} = x_p h_p + x_o h_o \quad (24)$$

$$s_{mix} = x_p s_p + x_o s_o - R(x_p \ln x_p + x_o \ln x_o) \quad (25)$$

The equilibrium fraction of P-hydrogen is solely dependent on temperature;[33] in particular, the change in the P-hydrogen fraction is the most drastic at 50 K, as shown in Figure 7. In this study, O-hydrogen and P-hydrogen were completely converted within the O−P converter, where the P-hydrogen fraction was determined by the temperature of the outlet hydrogen. Therefore, the conversion heat of the O-hydrogen and P-hydrogen was equal to the enthalpy difference between the inlet and outlet hydrogen within the O−P converter. Table 2 shows the P-hydrogen fraction of H_2 streams from feed to the product versus temperature. The calculation formula is as follows[41]

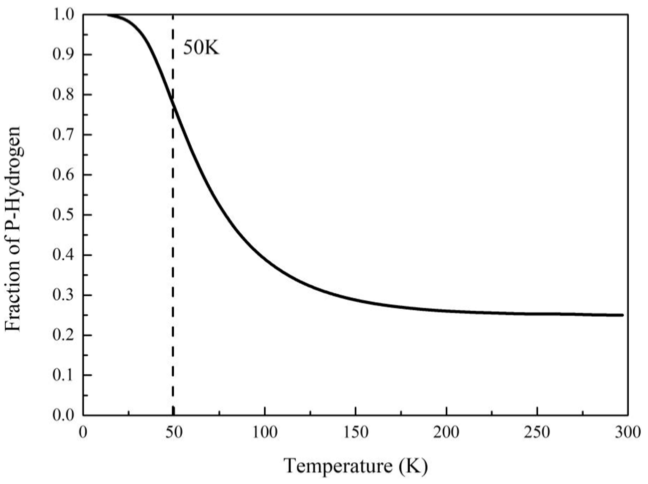

Figure 7. Fraction of P-hydrogen as a function of temperature.

https://doi.org/10.1021/acsomega.4c09299
ACS Omega 2025, 10, 8089−8102

Table 2. P-Hydrogen Fraction of H_2 Streams

stream ID	para (%)	stream ID	para (%)
H2−1	24.95	H2−8	65.37
H2−2	24.95	H2−9	65.37
H2−3	24.95	H2−10	77.04
H2−4	30.97	H2−11	77.04
H2−5	30.97	H2−12	77.04
H2−6	48.24	H2−13	95.18
H2−7	48.24	H2−14	95.18
LH2−1	95.18		

$$y_{H2,p} = 0.1\left[\exp\left(\frac{-5.313}{T/T_c}\right) + 0.1\right]^{-1} - 2.5 \times 10^{-4}\left(\frac{T}{T_c}\right)^3 + 3.7 \times 10^{-3}\left(\frac{T}{T_c}\right)^2 - 2.0 \times 10^{-3}\left(\frac{T}{T_c}\right) - 0.0027 \quad (26)$$

In the formula, $y_{H2,p}$ is the P-hydrogen mass fraction. T is the equilibrium hydrogen temperature in a specific state, K.

To provide a clear procedural overview, combining Section 2.1 (Process Description) and Section 2.2 (Methodology and Building), a flowchart of this research was drawn, which included the key process of hydrogen liquefaction and the corresponding equations and methodologies, as shown in Figure 8. In addition, this simulation model contains the unit equipment (heat exchanger, compressor, expander, and throttle valve) required for the gas liquefaction process, and it has flexibility to adapt to other gases liquefaction processes, such as natural gas.

3. RESULTS AND DISCUSSION

This section contains results of the simulation, energy, and exergy analysis of the proposed liquefaction system. First of all, energy analysis is explained; then, the exergy analysis is elaborated and discussed. Finally, the influences of compressor performance and system scale are presented and described.

3.1. Energy Analysis. According to the energy analysis of the liquefaction system, the energy consumption of the compressor, LN_2, ideal liquid hydrogen, and expander output power is shown in Figure 9. The compressor energy consumption was 171.43 kW, the LN_2 energy consumption was 43.15 kW, the expander output work was 9.89 kW, and the total energy consumption was 204.68 kW. Notably, the compressor was the main energy consumption source, accounting for 83.75% of total energy consumption. The SEC of the liquefaction system was 9.82 kW h/kg_{LH2}.

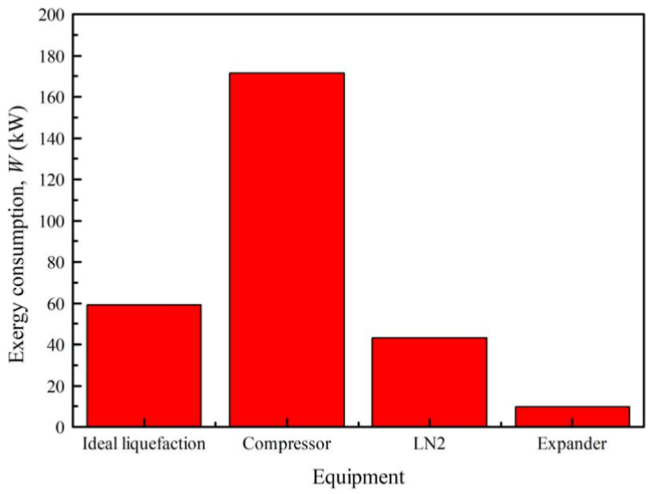

Figure 9. Energy consumption of the main part of the liquefaction system.

The greenhouse gas (GHG) emissions in hydrogen liquefaction come from three branches: refrigerant, infrastructure (capital goods), and electricity (operating). In Kim'

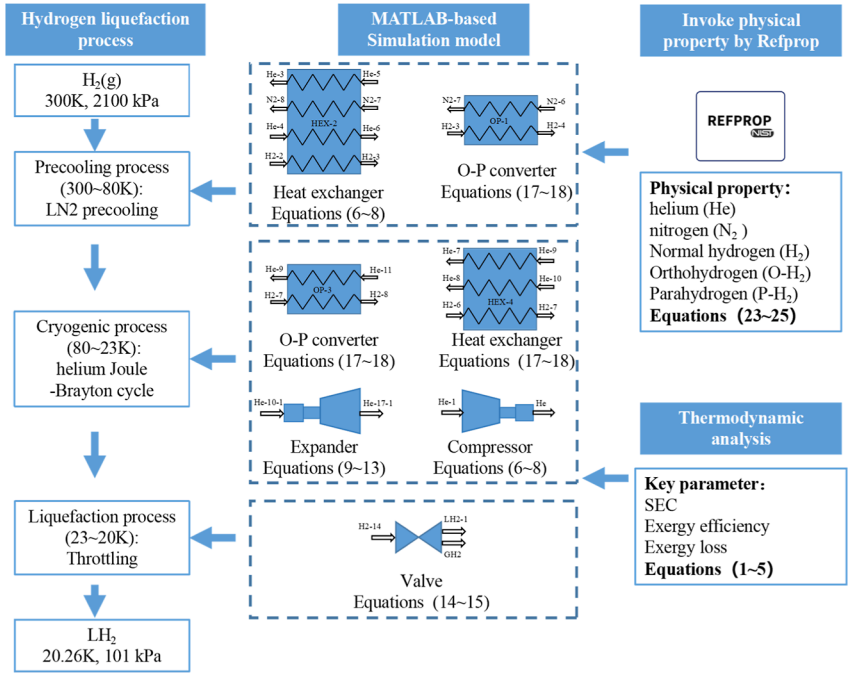

Figure 8. Flowchart of simulation model development in this study.

https://doi.org/10.1021/acsomega.4c09299
ACS Omega 2025, 10, 8089−8102

Table 3. Thermodynamic Parameters of Each Stream in the Liquefaction System

stream ID unit	temperature T (K)	pressure P (kPa)	mass flow m (kg/s)	mass enthalpy h (kJ/kg)	mass entropy s (kJ/kg K)	mass exergy e (kJ/kg K)	exergy flow E (kW)
				H_2 stream			
H2−1	300.00	2100	0.0058	4492.14	50.07	3769.31	21.81
H2−2	210.00	2100	0.0058	3219.88	45.03	4007.83	23.19
H2−3	130.00	2100	0.0058	2165.02	38.74	4842.13	28.02
H2−4	130.00	2100	0.0058	2133.38	38.53	4872.11	28.20
H2−5	80.00	2100	0.0058	1524.29	32.63	6032.15	34.91
H2−6	80.00	2100	0.0058	1405.87	31.42	6278.94	36.34
H2−7	60.00	2100	0.0058	1158.75	27.86	7099.79	41.09
H2−8	60.00	2100	0.0058	1038.68	26.11	7501.86	43.41
H2−9	50.00	2100	0.0058	900.88	23.60	8119.40	46.99
H2−10	50.00	2100	0.0058	819.04	22.11	8485.10	49.10
H2−11	39.00	2100	0.0058	595.71	16.97	9801.08	56.72
H2−12	33.00	2100	0.0058	352.58	10.26	11571.35	66.96
H2−13	33.00	2100	0.0058	226.57	7.23	12355.82	71.50
H2−14	20.00	2100	0.0058	50.66	0.70	14138.22	81.82
GH2	20.26	101	0.0002	479.94	23.25	7802.52	1.73
LH2−2	20.26	101	0.0002	33.65	1.23	13962.42	3.09
LH2−1	20.26	101	0.0056	33.65	1.23	13962.42	77.71
				He stream			
He	591.94	1200	0.1073	3082.99	26.41	2002.82	214.90
He-1	288.46	200	0.1073	1503.83	26.39	427.23	45.84
He-2	300.00	1200	0.1073	1567.02	22.88	1545.59	165.84
He-3	201.92	200	0.1073	1054.39	24.54	533.51	57.25
He-4	210.00	1200	0.1073	1099.52	21.02	1633.92	175.32
He-5	124.97	200	0.1073	654.69	22.05	881.47	94.58
He-6	130.00	1200	0.1073	683.60	18.53	1966.04	210.96
He-7	76.88	200	0.1073	404.75	19.52	1389.06	149.05
He-8	80.00	1200	0.1073	422.95	16.00	2464.81	264.47
He-9	53.27	200	0.1073	281.90	17.61	1838.93	197.32
He-10	59.10	1200	0.1073	313.43	14.41	2831.36	303.81
He-10−1	59.10	1200	0.0468	313.43	14.41	2831.36	132.58
He-10−2	59.10	1200	0.0605	313.43	14.41	2831.36	171.22
He-11	52.02	200	0.1073	275.43	17.49	1869.36	200.58
He-12	41.16	1200	0.0605	218.59	12.50	3310.47	200.20
He-12−1	41.16	1200	0.0240	218.59	12.50	3310.47	79.58
He-12−2	41.16	1200	0.0364	218.59	12.50	3310.47	120.62
He-13	40.34	200	0.1073	214.54	16.17	2206.10	236.71
He-14	39.00	1200	0.0364	207.06	12.21	3385.26	123.34
He-15	39.50	200	0.1073	210.13	16.06	2234.86	239.80
He-16	31.88	1200	0.0364	168.76	11.13	3672.36	133.81
He-17	36.44	200	0.1073	194.17	15.64	2345.07	251.63
He-17−1	36.44	200	0.0468	194.17	15.64	2345.07	109.81
He-17−2	36.44	200	0.0605	194.17	15.64	2345.07	141.82
He-18	19.48	200	0.0364	105.12	12.34	3243.22	118.17
He-19	27.59	200	0.0605	147.83	14.18	2735.84	165.45
He-21	25.29	200	0.0605	135.77	13.72	2860.70	173.00
He-21−1	25.29	200	0.0240	135.77	13.72	2860.70	68.77
He-21−2	25.29	200	0.0364	135.77	13.72	2860.70	104.23
He-23	19.90	200	0.0364	107.34	12.46	3211.62	116.77
				N_2 stream			
LN2−1	77.33	101	0.0745	5.20	4.48	403.02	30.02
LN2−2	77.33	101	0.0269	−121.93	2.84	769.08	20.71
N2−3	77.33	101	0.0476	77.14	5.41	195.85	9.32
N2−4	77.33	101	0.0269	−96.47	3.16	695.78	18.73
N2−5	77.33	101	0.0269	77.14	5.41	195.85	5.27
N2−6	77.33	101	0.0745	77.14	5.41	195.85	14.59
N2−7	79.52	101	0.0745	79.59	5.44	188.91	14.07
N2−8	178.83	101	0.0745	184.89	6.30	35.50	2.64
N2−9	298.61	101	0.0745	309.74	6.84	0.00	0.00

https://doi.org/10.1021/acsomega.4c09299
ACS Omega 2025, 10, 8089−8102

study,[42] the GHG emissions of the hydrogen liquefaction system were 67.85 kg CO_{2eq}/kg_{LH2}, mainly from one-time purchased refrigerants. The hydrogen liquefaction process proposed in this study did not use mixed refrigerants (methane, ethane, propane, etc.) and therefore had lower GHG emissions. The GHG emissions of electricity consumption (SEC = 9.82 kW h/kg_{LH2} @0.5 t/d) in this study, 5.47 kg CO_{2eq}/kg_{LH2}, were calculated based on the average grid carbon emission coefficient (0.557 $kgCO_2$/kW h) released by the National Bureau of Statistics of China according to its own power structure statistics. However, the GHG emissions of electricity consumption (SEC = 9.477 kW h/kg_{LH2} @1 t/d) in Kim' study were 0.26 kg CO_{2eq}/kg_{LH2}. The indirect carbon emission from using electricity depends on the type of electricity and whether it is renewable. Without a detailed description of the electricity source, these results are difficult to compare. Nevertheless, based on economic and environmental aspects, we believe that the proposed process has enough potential for large-scale applicability to meet the clean energy goals. In addition, the use of clean electricity to electrolyze water for hydrogen production and hydrogen liquefaction will further reduce carbon emissions.

The SEC of the liquefaction system was quite a low value compared to the current plant in Ingolstadt with an SEC of 13.58 kW h/kg_{LH2}[14] but slightly higher than that of the conceptual liquefaction system mentioned in the previous literature (5−7 kW h/kg_{LH2}) (18, 20, 21, 36). The primary factors contributing to this difference are as follows: First, the efficiency of the compressor and expander in this study was 70% and 75%, respectively, while in large-scale hydrogen liquefaction simulation (>50 t/d), the efficiency was typically set at 80% or above.[21,23] Second, ortho−parahydrogen conversion heat was considered in this study.

3.2. Exergy Analysis. Table 3 presents the thermodynamic properties of each stream in the liquefaction system. Figure 10

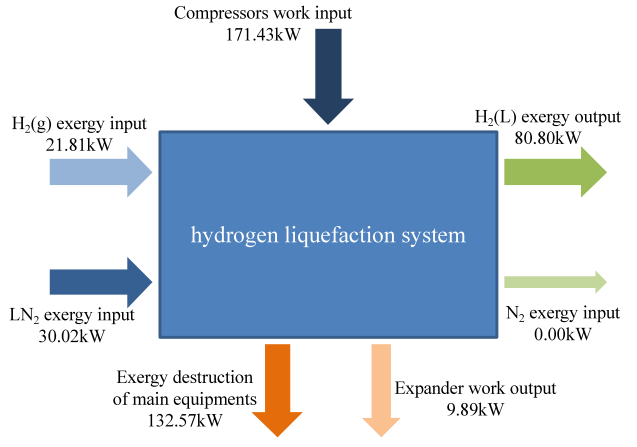

Figure 10. Various exergy input and output items in the liquefaction system.

shows various exergy input and output items in the liquefaction system. Notably, the highest input exergy flow was the compressor, 171.43 kW, and the second input exergy flow was LN_2, 30.02 kW, which were also the main source of energy consumption for the system. The output exergy flow mainly included the exergy destruction of equipment and liquid hydrogen. The exergy efficiency of the system was 28.82%, revealing that the proposed process had better thermodynamic performance than current processes, but there was still potential to improve the liquefaction process.[14]

Table 4 illustrates the exergy loss of each piece of equipment within the liquefaction system, including multistream heat exchangers, compressors, expanders, O−P converters, and throttle valve. Various types of exergy flow in the liquefaction system as a Sankey diagram are shown in Figure 11. Notably, a compressor had the highest exergy destruction with an energy loss ratio of 38.79%, and expanders had the second exergy destruction among other equipment. Furthermore, refer to Table 3, since the inlet and outlet pressures of three expanders were the same, the exergy losses of EXP-1, EXP-2, and EXP-3 were positively correlated with the flow rate. The exergy loss of the heat exchanger is related to heat-exchange temperature difference and flow rate.[43] The exergy loss of HEX-2 was the largest, 8.30 kW, accounting for 24.68% of the heat-exchange exergy loss. Because the four-stream heat exchanger, HEX-2, had the highest flow rate and the largest LMTD that reached 40 K. Some LMTDs are low, around 2 K. A low LMTD means a significant heat-transfer effect, which can reduce SEC and exergy loss and improve exergy efficiency. It does put forward a higher requirement for the heat exchanger. According to the Field Synergy Principle by Guo,[44] in a convective heat transfer, the field synergy of velocity and temperature could enhance the heat-transfer coefficient, and the field synergy of cold and hot fluid temperature could improve the heat-transfer efficiency. The enhancement of heat-transfer performance can be achieved through the optimization of heat exchanger design and manufacture, including refining the structural design, enhancing the thermal conductivity of materials, improving the temperature and velocity distributions, etc. With the commercial application of hydrogen liquefaction, the processing and manufacturing technologies of related equipment will be further improved.

Table 4. Exergy Loss of Each Equipment in the Liquefaction System

equip. ID	exergy loss (kW)	exergy loss ratio (%)	equip. ID	exergy loss (kW)	exergy loss ratio (%)
HEX-1	3.19	2.41	OP-1	0.34	0.26
HEX-2	8.30	6.26	OP-2	0.55	0.41
HEX-3	7.69	5.80	OP-3	0.94	0.71
HEX-4	4.19	3.16	OP-4	0.97	0.73
HEX-5	3.59	2.70	OP-5	3.01	2.27
HEX-6	1.49	1.12	EXP-1	17.19	12.96
HEX-7	2.93	2.21	EXP-2	8.82	6.65
HEX-8	2.22	1.67	EXP-3	13.32	10.05
HEX-9	0.04	0.03	COMP	51.43	38.79
VLV	2.38	1.80			

So the exergy loss of the heat exchanger could be reduced by the following methods: refining the design and manufacturing of heat exchangers, such as optimizing the structural design, enhancing the thermal conductivity of the material, improving the temperature and velocity field, etc., and optimizing the temperature distribution of cold and heat flows in the hydrogen liquefaction process.

Figure 12 shows the exergy loss of the main equipment in the liquefaction system. In fact, it depicts the total results of Table 4 and Figure 10 to get a quick overview of the irreversibility through total equipment. The exergy loss of the liquefaction system was 132.57 kW, while the exergy losses of

https://doi.org/10.1021/acsomega.4c09299
ACS Omega 2025, 10, 8089−8102

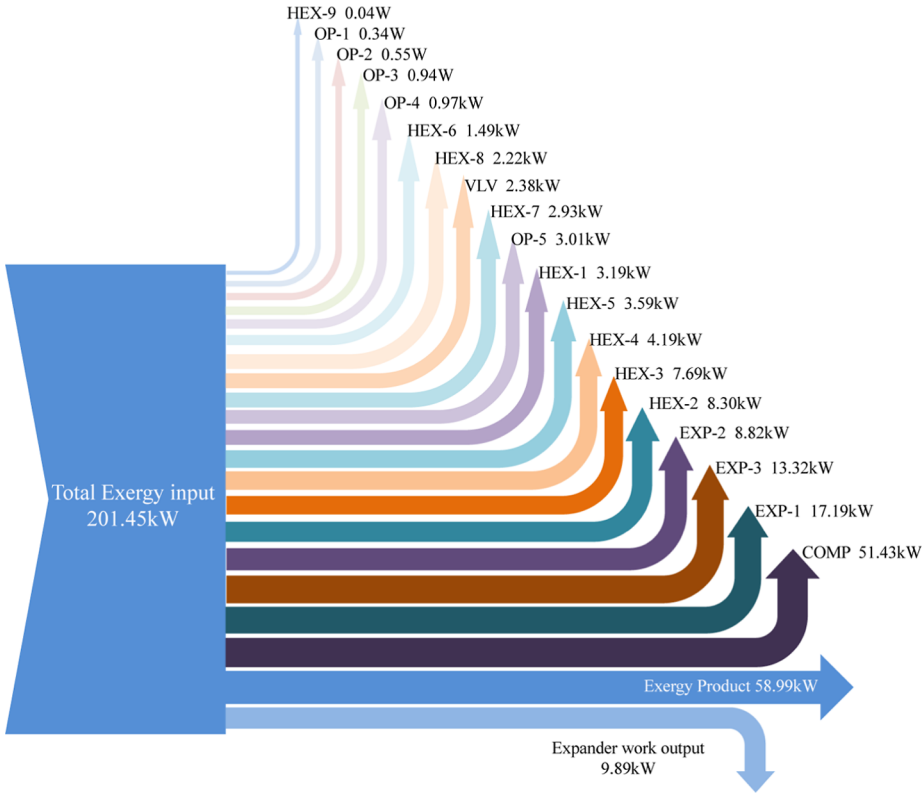

Figure 11. Various types of exergy flow in the liquefaction system.

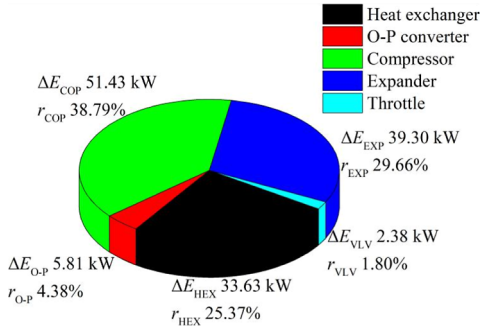

Figure 12. Exergy loss of the main equipment in the liquefaction system.

the heat exchanger, compressor, expander, O−P converter, and throttle were 33.63, 51.43, 39.33, 5.80, and 2.38 kW, respectively. For the compressor, expander, and heat exchanger, the overall exergy losses were at a quantitative level.

Specifically, compressors exhibited a loss of 38.79%, expanders recorded 29.66%, heat exchangers accounted for 25.37%, and the O−P converters and throttle contributed only 4.38% and 1.80%, respectively. Notably, compressors accounted for the largest share of exergy loss, followed by expanders and heat exchangers, which was consistent with Xiong's conclusion.[45] As a result, optimizing these three primary components, particularly compressors, held significant potential for enhancing exergy efficiency and minimizing energy consumption.[46,47]

In reality, there was always irreversibility in the various processes of the liquefaction system. The internal process of the helium compressor was irreversible compression.[47] Compressor design should maximize the compression efficiency, such as multistage compression and interstage cooling, to reduce exergy loss.[45] The primary source of exergy loss in the heat exchanger was in the temperature gradient between the internal cold and hot fluids, as well as the heat exchange that occurred between the exchanger and its surroundings. Therefore, reducing the temperature difference between the cold and hot fluids, as well as improving the adiabatic capacity of the liquefaction system, such as high vacuum insulated cold box, were the main measures to reduce the exergy loss of the heat exchanger.[48] The primary source of exergy loss in the expander laid in the internal irreversible process, which was related to many factors such as enthalpy drop, flow rate, impeller size, and working temperature of the expander. Enhancing the isentropic efficiency of the expander was crucial in reducing the total exergy loss, such as adjusting the flow through part of the expansion process to reduce flow loss and optimizing the cold end structure of the expander to avoid large heat leakage.[45]

3.3. Analysis of Influence Factors. Given the pivotal role of the compressor in the liquefaction system, which accounted for the largest share of energy consumption and exergy loss, the influence of helium compressor efficiency on both SEC and exergy efficiency was analyzed. As depicted in Figure 13, a notable and linear upward trend in exergy efficiency was observed. Specifically, as the compressor efficiency rose from 65% to 90%, the exergy efficiency experienced a substantial increase, climbing from 27.07% to 35.41%. Concurrently, the SEC decreased from 10.46 to 8.00 kW h/kg_{LH2}. The energy consumption of the hydrogen liquefaction system mainly came from the compressor. This trend accorded with the expectation and quantified the impact of compressor on the system, which validated the rationality of the simulation.

https://doi.org/10.1021/acsomega.4c09299
ACS Omega 2025, 10, 8089−8102

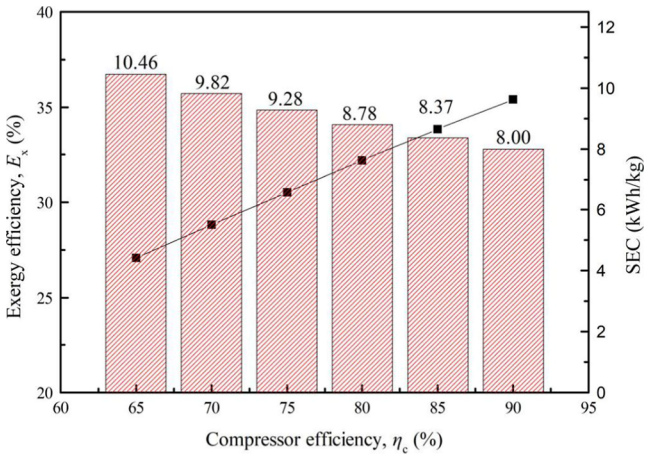

Figure 13. Impact of helium compressor efficiency on SEC and exergy efficiency.

Figure 14 illustrates the influence of compressor efficiency on the exergy loss ratio of the main equipment. With the improvement of compressor efficiency, the exergy loss ratio of the compressor exhibited a linear decline trend, whereas the exergy loss ratio of other equipment increased. Specifically, the heat-exchanger HEX-1, positioned downstream of the compressor (COMP), effectively reduced the outlet stream (He) to room temperature. Subsequently, the temperature and pressure at the outlet stream (He-2) remained constant at 210 K and 1.2 MPa, respectively. It indicated that the stream parameters of the subsequent process were not affected by the compressor efficiency. However, there was a notable change in the energy consumption and exergy loss of the compressor itself, whereas other equipment in the system remained unaffected.

It was widely acknowledged in the research community that scaling up the hydrogen liquefaction system could lead to significant reduction in SEC. That was attributed to the enhanced efficiency of equipment such as compressors and expanders, as well as reducing relative leakage losses.[49,50] Furthermore, the SEC and exergy loss of the 50 t/day hydrogen liquefaction system were analyzed in this study. Notably, as the system's scale increased, the efficiency of both

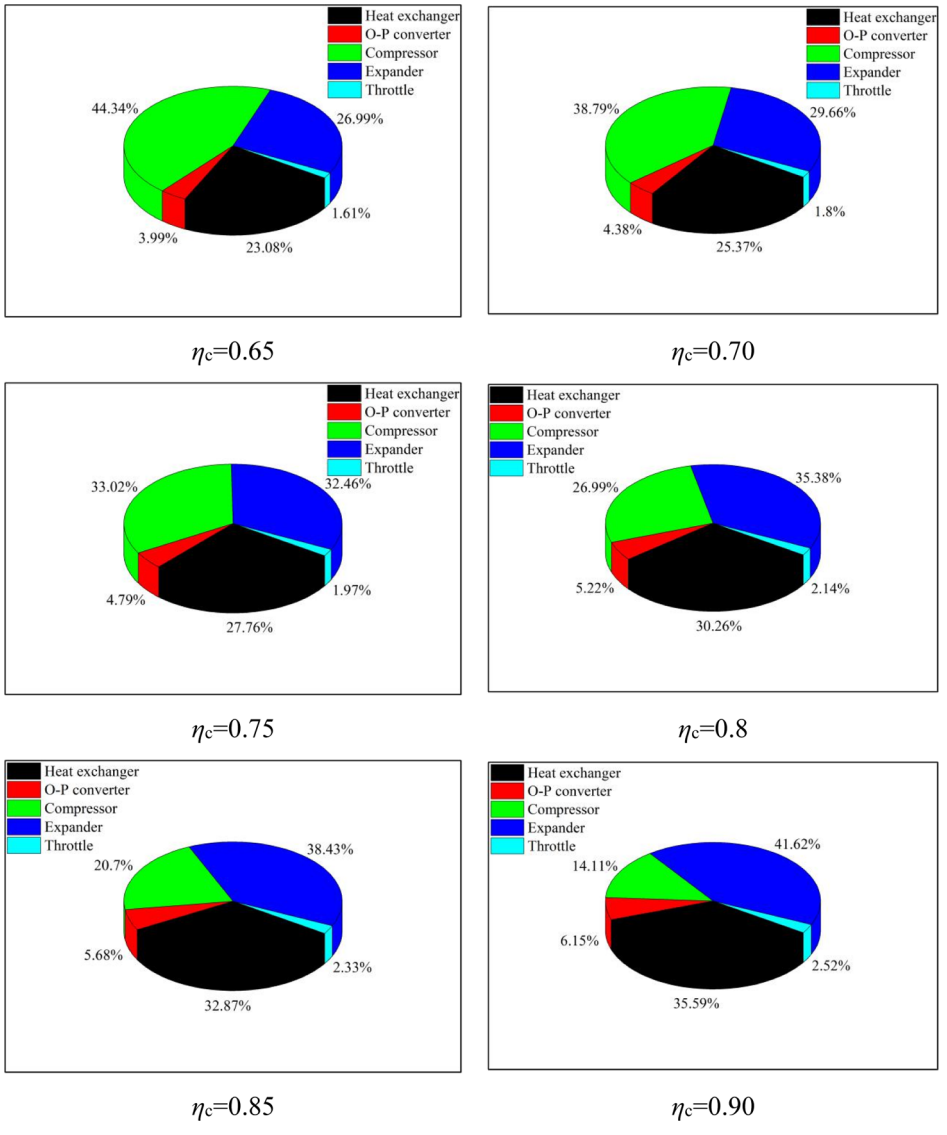

Figure 14. Impact of compressor efficiency on the exergy loss ratio of the main equipment.

https://doi.org/10.1021/acsomega.4c09299
ACS Omega 2025, 10, 8089−8102

the compressor and the expander exhibited a positive trend. Compared with the 0.5 t/d case, the compressor and expander efficiency in the 50 t/d case were set to 80% and 85%, respectively, and other parameters are consistent with Table 1. The simulation result showed that, in the 50 t/d case, the SEC of the liquefaction system was 7.35 kW h/kg_{LH2}, while the exergy efficiency was 38.45%. The corresponding carbon emission was 4.09 kg of CO_{2eq}/kg_{LH2}.

Figure 15 shows the exergy loss of the main equipment in the liquefaction system. A statistical analysis revealed that the

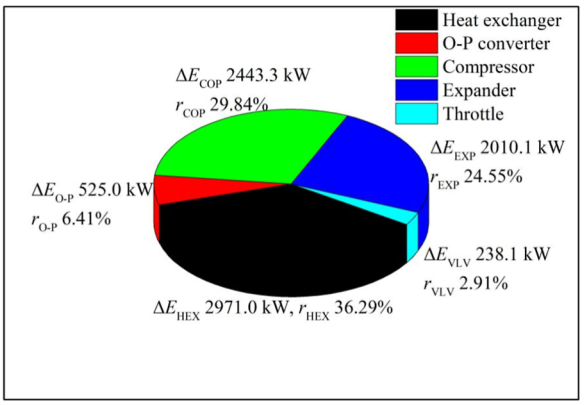

Figure 15. Exergy loss of the main equipment in the liquefaction system.

exergy loss of the liquefaction system was 8187.65 kW, while the exergy losses of the compressor, expander, heat exchanger, O−P converter, and throttle were 2443.34, 2010.11, 2971.03, 525.03, and 238.14 kW, respectively. Specifically, the exergy losses of the compressor, expander, heat exchanger, O−P converter, and throttle were 29.84%, 24.55%, 36.29%, 6.41%, and 2.91%, respectively.

In comparison to the 0.5 t/d system, the exergy loss of the compressor and expander in the 50 t/d system exhibited a reduction, with the heat exchanger's exergy loss emerging as the primary contributor. This was mainly due to improvement of the efficiency of the mechanical equipment. Compared with the exergy loss of 33.6 kW in the 0.5 t/d system, the exergy loss of the heat exchanger in the 50 t/d system was 2971.0 kW, which did not increase proportionately. That was attributed to the better temperature distribution of cold and heat flows throughout the system and the smaller heat-transfer temperature difference. In the heat exchanger, the better the field synergy of cold and hot fluids, that is, the reasonable fluid organization and uniform temperature difference field, the higher the heat-transfer efficiency. By optimizing the temperature distribution of cold and heat flows in the hydrogen liquefaction process, the matching between hot and cold composite curves within the heat exchanger could be improved, reducing irreversible loss caused by the temperature difference. This was a large optimization space in the design of the hydrogen liquefaction process, which was also mentioned in Sadaghiani's and Ansarinasab's studies.[23,46] Therefore, in the development of large-scale hydrogen liquefaction, minimizing exergy loss during the heat-exchange process served as a significant research direction for enhancing exergy efficiency and reducing SEC.

4. CONCLUSIONS

In this study, an independent hydrogen liquefaction simulation model and simulation program based on MATLAB and REFPROP were built, and a hydrogen liquefaction process with LN2 precooling and helium Joule−Brayton cryogenic cycle was proposed. Furthermore, the effects of the liquefaction scale and compressor efficiency on the overall thermodynamic performance of the system were analyzed, providing reference for the development of hydrogen liquefaction equipment. The key conclusions are outlined below:

1. The equipment model and exergy analysis model in the hydrogen liquefaction system (including a compressor, a heat exchanger, an expander, an O−P converter, a throttle valve, etc.) were constructed, and ortho−parahydrogen conversion heat and the physical properties of equilibrium hydrogen were calculated. Finally, the independently built simulation program has achieved the simulation and analysis of the hydrogen liquefaction system successfully. The accuracy of simulation results was validated against commercial software Unisim Design.
2. For the 0.5 t/d hydrogen liquefaction system, the SEC was 9.82 kW h/kg_{LH2}, while the exergy efficiency was 28.82%. The compressor had the highest power loss ratio of 38.79%. The increase of compressor efficiency could improve exergy efficiency and reduce SEC significantly.
3. Compared with the 0.5 t/d case, the exergy losses of the compressor and expander decreased in the 50 t/d case, and the exergy loss of heat exchanger became the primary contributor, accounting for 36.29%. In the development of large-scale hydrogen liquefaction, refining heat-transfer performance and optimizing the temperature distribution of cold and heat flows in the hydrogen liquefaction process were the significant direction to improve exergy efficiency and reduce SEC.

AUTHOR INFORMATION

Corresponding Author

Wenhao Song − *State Grid Shandong Electric Power Research Institute, Ji Nan 250003, China*; orcid.org/0009-0006-7866-1978; Phone: +86 053067983708; Email: songwenhao0101@163.com

Authors

Ke Liu − *State Grid Shandong Electric Power Research Institute, Ji Nan 250003, China*

Zhonghua Zhao − *State Grid Shandong Electric Power Research Institute, Ji Nan 250003, China*

Limeng Zhang − *State Grid Shandong Electric Power Research Institute, Ji Nan 250003, China*

Xinguang Dong − *State Grid Shandong Electric Power Research Institute, Ji Nan 250003, China*

Xingsen Yang − *State Grid Shandong Electric Power Research Institute, Ji Nan 250003, China*

Chunxiao Tian − *State Grid Shandong Electric Power Research Institute, Ji Nan 250003, China*

Shuai Liu − *State Grid Shandong Electric Power Research Institute, Ji Nan 250003, China*

Shuo Cao − *State Grid Shandong Electric Power Research Institute, Ji Nan 250003, China*

Complete contact information is available at:

https://doi.org/10.1021/acsomega.4c09299
ACS Omega 2025, 10, 8089−8102

https://pubs.acs.org/10.1021/acsomega.4c09299

Author Contributions

Wenhao Song: Conceptualization, formal analysis, methodology, software, and writing—original draft, review, and editing; **Ke Liu**: Methodology, software, and writing—review and editing; **Zhonghua Zhao**: Formal analysis and writing—review and editing; **Limeng Zhang**: Supervision and validation; **Xinguang Dong**: Project administration and validation; **Xingsen Yang**: Project administration and Conceptualization; **Chunxiao Tian**: Data curation; **Shuai Liu**: Investigation; and **Shuo Cao**: Investigation.

Notes

The authors declare no competing financial interest.

■ ACKNOWLEDGMENTS

This study was funded by Shandong Postdoctoral Science Foundation (SDCX-ZG-202400202) and State Grid Shandong Electric Power Research Institute Foundation (ZY-2024-10).

■ NOMENCLATURE SYMBOLS SUBSCRIPTS

h: specific enthalpy kJ/kg; *s*: specific entropy, kJ/(kg·K); *T*: temperature, K; *P*: pressure; *e*: specific exergy, kJ/kg; *E*: the rate of exergy flow, kW; E_x: exergy efficiency; c_p: specific heat, kJ/(kg·K); *r*: ratio; *W*: power, kW; *m*: mass flow rate, kg/s; Δ: gradient; *η*: efficiency of equipment; a: environmental state; in: inlet; out: outlet; c: cold; h: hot; co: compressor; ex: expander; O: ortho; P: para; *i*: equipment *i*; *j*: equipment *j*; 1, 2, ... to *n*: 1, 2, ... to *n*/of stream numbers

■ REFERENCES

(1) Pivovar, B.; Rustagi, N.; Satyapal, S. Hydrogen at scale (H2@ Scale): key to a clean, economic, and sustainable energy system. *Electrochem. Soc. Interface* **2018**, *27* (1), 47.
(2) DOE *National Clean Hydrogen Strategy and Roadmap*, 2023.
(3) Alliance, C. H. *China Hydrogen Energy and Fuel Cell Industry Development Report 2020*, 2021.
(4) Government Tomorrow Forum *International Hydrogen Strategies*, 2020.
(5) NEDO J *Hydrogen Energy White Paper*, 2015.
(6) Lemmon, E.; Huber, M. L.; Mclinden, M. O. *NIST Standard Reference Database 23: Reference Fluid Thermodynamic and Transport Properties-REFPROP, version 80*; NIST, 2007.
(7) Decker, L. Overview on cryogenic refrigeration cycles for large scale HTS applications. In *IOP Conference Series: Materials Science Engineering*; IOP Science, 2016.
(8) Peschka, W. *Liquid Hydrogen: Fuel of the Future*; Springer Science & Business Media, 1992.
(9) Nandi, T. K.; Sarangi, S. Performance and optimization of hydrogen liquefaction cycles. *Int. J. Hydrogen Energy* **1993**, *18* (2), 131−139.
(10) Krasae-In, S.; Stang, J. H.; Neksa, P. Exergy analysis on the simulation of a small-scale hydrogen liquefaction test rig with a multi-component refrigerant refrigeration system. *Int. J. Hydrogen Energy* **2010**, *35* (15), 8030−8042.
(11) Timmerhaus, K. D.; Flynn, T. M. *Cryogenic Process Engineering*; Springer Science & Business Media, 2013.
(12) Yang, X.; Yang, C. Study on performance of orthohydrogen-parahydrogen converting catalyst. *Chem. Propellants Polym. Mater* **2018**, *16* (3), 79−92.
(13) Donaubauer, P. J.; Cardella, U.; Decker, L.; Klein, H. Kinetics and Heat Exchanger Design for Catalytic Ortho-Para Hydrogen Conversion during Liquefaction. *Chem. Eng. Technol.* **2019**, *42* (3), 669−679.
(14) Bracha, M.; Lorenz, G.; Patzelt, A.; Wanner, M. Large-scale hydrogen liquefaction in Germany. *Int. J. Hydrogen Energy* **1994**, *19* (1), 53−59.
(15) Ohira, K. *A Summary of Liquid Hydrogen and Cryogenic Technologies in Japan's WE-NET Project*; American Institute of Physics, 2004; Vol. *710*, pp 27−34.
(16) Ohlig, K.; Decker, L. The latest developments and outlook for hydrogen liquefaction technology. In *AIP Conference Proceedings*; American Institute of Physics, 2014.
(17) Garceau, N. M.; Baik, J. H.; Lim, C. M.; Kim, S.; Oh, I. H.; Karng, S. W. Development of a small-scale hydrogen liquefaction system. *Int. J. Hydrogen Energy* **2015**, *40* (35), 11872−11878.
(18) Yin, L.; Ju, Y. Review on the design and optimization of hydrogen liquefaction processes. *Front. Energy* **2020**, *14*, 530−544.
(19) Kuz'Menko, I. F.; Morkovkin, I. M.; Gurov, E. I. Concept of Building Medium-Capacity Hydrogen Liquefiers with Helium Refrigeration Cycle. *Chem. Petrol. Eng.* **2004**, *40* (1), 94−98.
(20) Belyakov, V. V.; Krakovskii, B. D.; Popov, O. M.; Step, G. K.; Udut, V. N. Low-Capacity Hydrogen Liquefier with a Helium Cycle. *Chem. Petrol. Eng.* **2002**, *38* (3/4), 150−153.
(21) Valenti, G.; Macchi, E. Proposal of an innovative, high-efficiency, large-scale hydrogen liquefier. *Int. J. Hydrogen Energy* **2008**, *33* (12), 3116−31212.
(22) Lianpeng, Z.; Zhenyang, Z.; Gang, A.; Shenyin, Y. Progress in hydrogen liquefaction technology with mixed refrigerant. *Power Gener. Technology* **2023**, *44* (03), 331−339.
(23) Sadaghiani, M. S.; Mehrpooya, M. Introducing and energy analysis of a novel cryogenic hydrogen liquefaction process configuration. *Int. J. Hydrogen Energy* **2017**, *42* (9), 6033−6050.
(24) Zhang, S.; Liu, G. Design and performance analysis of a hydrogen liquefaction process. *Clean Technol. Environ. Policy* **2022**, *24*, 51−65.
(25) Bi, Y.; Ju, Y. Conceptual design and optimization of a novel hydrogen liquefaction process based on helium expansion cycle integrating with mixed refrigerant pre-cooling. *Int. J. Hydrogen Energy* **2022**, *47* (38), 16949−16963.
(26) Faramarzi, S.; Nainiyan, S. M. M.; Mafi, M.; Ghasemiasl, R. A novel hydrogen liquefaction process based on LNG cold energy and mixed refrigerant cycle. *Int. J. Refrig.* **2021**, *131*, 263−274.
(27) Ansarinasab, H.; Mehrpooya, M.; Sadeghzadeh, M. An exergy-based investigation on hydrogen liquefaction plant-exergy, exergoeconomic, and exergoenvironmental analyses. *J. Clean. Prod.* **2019**, *210*, 530−541.
(28) Naquash, A.; Riaz, A.; Lee, H.; Qyyum, M. A.; Lee, S.; Lam, S. S.; et al. Hydrofluoroolefin-based mixed refrigerant for enhanced performance of hydrogen liquefaction process. *Int. J. Hydrogen Energy* **2022**, *47* (98), 41648−41662.
(29) Quack, H. Conceptual design of a high efficiency large capacity hydrogen liquefier. In *AIP Conference Proceedings*; American Institute of Physics, 2002.
(30) Wu, Y.; Li, Y. *Refrigeration and Cryogenic Devices*; Higher Education Press: Bei Jing, 2009.
(31) Voth, R. O. Studies of Hydrogen Liquefier Efficiency and the Recovery of the Liquefaction Energy. In *Cryogenics Division*; National Bureau of Standards, 1977.
(32) Staats, W. L. *Analysis of a Supercritical Hydrogen Liquefaction Cycle*; Georgia Institute of Technology, 2008.
(33) Yang, J. H.; Yoon, Y.; Ryu, M.; An, S. K.; Shin, J.; Lee, C. J. Integrated hydrogen liquefaction process with steam methane reforming by using liquefied natural gas cooling system. *Appl. Energy* **2019**, *255*, 113840.
(34) Valenti, G.; Macchi, E.; Brioschi, S. The influence of the thermodynamic model of equilibrium-hydrogen on the simulation of its liquefaction. *Int. J. Hydrogen Energy* **2012**, *37* (14), 10779−10788.
(35) Choi, J. W.; Kim, Y.; Lee, K.; Kim, H.; Han, K.; Park, J. *Liquid Hydrogen Properties*; Korea Atomic Energy Research Institute, 2004.
(36) Lara, Y.; Petrakopoulou, F.; Morosuk, T.; Boyano, A.; Tsatsaronis, G. An exergy-based study on the relationship between

costs and environmental impacts in power plants. *Energy* **2017**, *138* (1), 920−928.
(37) Aslambakhsh, A. H.; Moosavian, M. A.; Amidpour, M.; Hosseini, M.; Amirafshar, S. Global cost optimization of a mini-scale liquefied natural gas plant. *Energy* **2018**, *148* (1), 1191−1200.
(38) Nazari, F.; Jin, Y. C.; Shakibaeinia, A. Numerical analysis of jet and submerged hydraulic jump using moving particle semi-implicit method. *Can. J. Civ. Eng.* **2012**, *39* (5), 495−505.
(39) Carrillo, J. M.; Marco, F.; Castillo, L. G.; García, J. T. Experimental study of submerged hydraulic jumps generated downstream of rectangular plunging jets. *Int. J. Multiphase Flow* **2021**, *137* (5), 103579.
(40) Yuksel, Y. E.; Ozturk, M.; Dincer, I. Analysis and assessment of a novel hydrogen liquefaction process. *Int. J. Hydrogen Energy* **2017**, *42* (16), 11429−11438.
(41) Xu, P.; Wen, J.; Li, Y.; Wang, S.; Tu, J. Study on Hydrogen Ortho-Para Conversion Couple with Flow and Heat Transfer of the Plate Fin Heat Exchanger. *J. Xi'an Jiaot. Univ.* **2021**, *55* (12), 16−24.
(42) Kim, H.; Haider, J.; Qyyum, M. A.; Lim, H. Mixed refrigerant−based simplified hydrogen liquefaction process: Energy, exergy, economic, and environmental analysis. *J. Clean. Prod.* **2022**, *367*, 132947.
(43) Yin, L.; Ju, Y. Process optimization and analysis of a novel hydrogen liquefaction cycle. *Int. J. Refrig.* **2020**, *110*, 219−230.
(44) Guo, Z. Field synergy principle in heat exchanger and its application. *Chin. J. Mech. Eng.* **2003**, *39* (12), 1−9.
(45) Xiong, L.; Yang, K.; Kong, W.; Yang, Z.; Zhu, J.; Zhou, G.; et al. Development of a 5 t/d Hydrogen Liquefaction Unit. *Vacuum and Cryogenics* **2024**, *30* (04), 349−354.
(46) Ansarinasab, H.; Mehrpooya, M.; Mohammadi, A. Advanced exergy and exergoeconomic analyses of a hydrogen liquefact ion plant equipped with mixed refrigerant system. *J. Clean. Prod.* **2017**, *144* (15), 248−259.
(47) Asadnia, M.; Mehrpooya, M. A novel hydrogen liquefaction process configuration with combined mixed refrigerant systems. *Int. J. Hydrogen Energy* **2017**, *42* (23), 15564−15585.
(48) Zheng, P.; An, G. Exergy analysis of a cryogenic liquefaction plant. *Cryogenics* **2010**, *2010* (01), 28−32.
(49) Cardella, U.; Decker, L.; Klein, H. Economically viable large-scale hydrogen liquefaction. *IOP Conf. Ser.:Mater. Sci. Eng.* **2017**, *171* (1), 012013.
(50) Cardella, U.; Decker, L.; Klein, H. Roadmap to economically viable hydrogen liquefaction. *Int. J. Hydrogen Energy* **2017**, *42* (19), 13329−13338.

https://doi.org/10.1021/acsomega.4c09299
ACS Omega 2025, 10, 8089−8102